Hydroxyl radical reactions with 4-chlorophenol as a model for heterogeneous photocatalysis

ARTICLE *in* JOURNAL OF MOLECULAR STRUCTURE THEOCHEM · FEBRUARY 2008

Impact Factor: 1.37 · DOI: 10.1016/j.theochem.2007.11.022

2 AUTHORS:

Murat Kılıç
Erciyes Üniversitesi
10 PUBLICATIONS **94** CITATIONS
SEE PROFILE

Zekiye Cinar
Yildiz Technical University
27 PUBLICATIONS **439** CITATIONS
SEE PROFILE

ELSEVIER

Journal of Molecular Structure: THEOCHEM 851 (2008) 263–270

THEO CHEM

www.elsevier.com/locate/theochem

Hydroxyl radical reactions with 4-chlorophenol as a model for heterogeneous photocatalysis

Murat Kılıç, Zekiye Çınar *

Department of Chemistry, Yıldız Technical University, 34220 Istanbul, Turkey

Received 10 July 2007; received in revised form 14 November 2007; accepted 14 November 2007
Available online 24 November 2007

Abstract

In this study, with the intention of determining the primary intermediates, the photocatalytic degradation reaction of 4-chlorophenol (4-CP) which has been accepted as the standard pollutant was modelled. Geometry optimizations of the reactants, the product radicals, the pre-reactive and the transition state complexes were performed for all the possible reaction paths. The DFT calculations were carried out by the hybrid B3LYP functional, which combines HF and Becke exchange terms with the Lee–Yang–Parr correlation functional by using 6-31G* basis set. The solvation effects were computed by using COSMO as the solvation model. Based on the results of the quantum mechanical calculations, the rate constants for all the possible reaction paths were calculated by means of the Transition State Theory. The difference in the rates of reaction paths were explained in terms of the presence of hydrogen bonds in the transition state complexes. The product distribution for the photocatalytic degradation of 4-CP was predicted. The results show that the major intermediates of the photocatalytic degradation of 4-CP are 4-chlorocatechol (4-CC) and hydroquinone (HQ) with [4-CC]>[HQ]. 4-Chlorophenoxyl radical which causes the formation of polyaromatics is not produced in either gas or aqueous phases.

Keywords: 4-Chlorophenol; Hydroxyl radicals; Heterogeneous photocatalysis; DFT calculations; COSMO method

1. Introduction

Due to their high toxicity to living organisms, bioaccumulation, strong odor emission and persistence in the environment, chlorinated aromatic compounds constitute an important class of water and air contaminants. Chlorinated phenols are widely used in industry and in daily life. They pose severe problems to the environment, because they are carcinogens and mutagens. These contaminants are generated from a number of industrial manufacturing processes such as pesticide, paint, solvent, pharmaceutical, wood preserving chemicals, coke-oven and pulp industries [1]. Due to their stability and solubility in water, chlorinated phenols are commonly present in industrial wastewater. There are many conventional methods to destroy such hazardous compounds. But, each method has its shortcomings. Chemical oxidation methods are expensive and chlorinated phenols are known to withstand biodegradation [2,3]. Photolytic oxidation processes, such as UV/ozone, UV/H_2O_2 or UV/perchlorate have been proven to be successful in destroying many toxic pollutants in wastewater. However, highly toxic products such as dibenzo-*p*-dioxins and polychlorinated dibenzofurans are formed during the UV-treatment of chlorinated aromatics [4]. Therefore, in recent years attention has been directed towards heterogeneous photocatalysis in order to avoid these highly toxic pollutants.

Heterogeneous photocatalysis is based on the combined use of low energy UV-A light and semiconductor photocatalysts. The anatase form of TiO_2 is the current preferred semiconductor, since it is inexpensive, non-toxic, chemically and biologically inert and commercially available. The most important feature of this new advanced oxidation process is the generation of the $^{\bullet}OH$ radicals upon irradiation. Band-gap excitation of TiO_2 (~3.2 eV) generates

* Corresponding author. Tel.: +90 212 449 1844; fax: +90 212 449 1514.
E-mail address: cinarz@yildiz.edu.tr (Z. Çınar).

0166-1280/$ - see front matter © 2007 Elsevier B.V. All rights reserved.
doi:10.1016/j.theochem.2007.11.022

electron–hole pairs that can initiate redox reactions on the surface of TiO_2 particles. The oxidation reactions of the adsorbed OH^- ions or H_2O molecules with the photogenerated holes yield ·OH radicals which can degrade a great variety of organic compounds [5–7].

The photocatalytic degradation of chlorinated phenols in TiO_2 suspensions have been studied by many investigators [3,4,8–12]. The results show that phenolic compounds decompose completely to CO_2 and H_2O through a mechanism involving hydroxylation of the aromatic ring. The substitution of the –OH group occurs at the *para* and/or *ortho* sites with respect to the phenolic functionality. This finding indicates that the reactions of phenols with the photogenerated ·OH radicals are the primary steps in their photodegradation mechanisms. The photocatalytic degradation reactions of chlorinated aromatics may take place through the formation of harmful intermediates such as polyaromatics that are more toxic than the original compound. Therefore, knowledge on the identities of the intermediates is a necessity in such processes.

4-Chlorophenol (4-CP) has been accepted as the standard pollutant for heterogeneous photocatalysis. The photocatalytic degradation of 4-CP has been the topic of many investigations [12–16]. The successful mineralization of 4-CP to CO_2 has been demonstrated, and in a number of studies intermediates have been identified and quantified. However, in some of these photocatalytic studies hydroquinone (HQ) was found to be the predominant aromatic intermediate, while in others 4-chlorocatechol (4-CC) was predominant. Stafford et al. [12] have demonstrated that 4-CC and HQ are the predominant intermediates formed when 4-CP was degraded in conditions favoring ·OH attack. A variety of mechanisms has been proposed to explain these observed results, however almost nothing is known about the mechanism of the photocatalytic degradation reaction of 4-CP.

In our previous study, we modeled the reactions of ·OH radicals with phenol derivatives theoretically by means of a semiempirical quantum chemical method, PM3, and determined that *ortho*-addition yielding 1,2-dihydroxy-4-chlorobenzene (4-chlorocatechol) is the dominant reaction path for 4-CP in both gas and aqueous media [17]. *Ipso*-addition was found to be less important than the *ortho*-addition which is in perfect agreement with several experimental results reported in the literature. In this paper, we focused on describing the mechanism of the photocatalytic degradation reaction of 4-CP in detail and explain the observed experimental results and differences. With this aim, we modeled the reaction 4-CP + ·OH by means of a more sophisticated quantum chemical method, Density Functional Theory, in order to determine the identities and the relative concentrations of the primary intermediates. Furthermore, the kinetics of the reaction and the effect of solvent water were investigated theoretically.

2. Methodology

In this study, reactions between ·OH radicals and 4-CP were modeled, including ·OH radical additions to the aromatic ring and direct H-atom abstraction from the phenolic functionality. Geometry optimizations of the reactants, the product radicals, pre-reactive and the transition state complexes were performed with the density functional theory (DFT) method within the GAUSSIAN 03 package [18], in order to take the electron correlation into account. The DFT calculations were performed by the hybrid B3LYP functional, which combines HF and Becke exchange terms with the Lee–Yang–Parr correlation functional by using 6-31G* basis set [19,20]. Zero point corrections for the energies were made and the thermodynamic properties of all the species involved in the reactions were calculated. In the calculation of the hydroxylated radicals, the aromatic ring was left planar except the position of attack and the attacking ·OH radical was assumed to form a tetrahedral angle with the C—H bond. The most stable conformer for each of the reactants and the products was determined by carrying out a conformer search [21,22].

Vibrational frequencies were calculated for the determination of the reactant and the product structures as stationary points and true minima on the potential energy surfaces. All possible stationary geometries located as minima were generated by free rotation around single bonds. The forming C—O bonds in the addition paths and the H—O bonds in the abstraction path were chosen as the reaction coordinates in the determination of the transition states and each transition state was characterized with only one negative eingenvalue in its force constant matrix.

The most interesting point obtained in this study is that the energies of the transition states, optimized with the DFT/B3LYP/6-31G* method are lower than the energies of the reactants, 4-CP and the ·OH radical. This finding indicates that in all the reaction paths, pre-reactive complexes which lower the total energy are formed before the formation of the transition state complexes. Therefore, pre-reactive complexes were located on the potential energy surfaces and characterized with positive eigenvalues in their force constant matrices.

In aqueous media, water molecules affect the energetics of the photocatalytic degradation reactions of all organic compounds. Moreover, water molecules induce geometry relaxation on the solute molecules. This effect on the geometry relaxation becomes more important when hydrogen bonded complexes are present. However, the results obtained in earlier studies indicate that geometry changes have a negligible effect on the energy of the solute in water for both open and closed shell structures [23,24]. Therefore, in this study, in order to take the effect of solvent H_2O on the energetics and the kinetics of the 4-CP + ·OH reactions into account, DFT/B3LYP/6-31G* calculations were carried out for the optimized structures of the reactants, the pre-reactive and the transition state complexes and the product radicals using COSMO (conductor-like screening

solvation model) [23] as the solvation model implemented in GAUSSIAN 03 package. The solvent was water at 25 °C with dielectric constant $\varepsilon = 78.39$.

COSMO is one of the polarizable continuum methods (PCMs). In PCMs, the solute molecule is placed in a cavity surrounded by a polarizable continuum whose reaction field modifies the energy and the properties of the solute [25]. The geometry of the cavity is determined by the shape of the solute. The reaction field is described in terms of apparent polarization charges or reaction field factors included in the solute Hamiltonian, so that it is possible to perform iterative procedures leading to the self – consistence between the solute wavefunction and the solvent polarization. The COSMO method describes the solvent reaction field by means of apparent polarization charges distributed on the cavity surface, which are determined by imposing that the total electrostatic potential cancels out on the surface. This condition can describe the solvation in polar liquids. Hence, it is the method of choice in this study.

3. Results and discussion

3.1. Reaction paths

The hydroxyl radical is a very active species and has a strong electrophilic character [26]. Once formed, it can readily attack 4-CP molecule and produce the reaction intermediates. ·OH radical reactions with aromatic compounds proceed by two reaction pathways; H-atom abstraction from C—H or O—H bonds and addition to aromatic rings. Four different reaction paths for the reaction of 4-CP with the ·OH radical were determined by nature of the carbon atoms of the aromatic ring and the functional —OH group. The first three of the reaction paths, *ortho*-addition (*o*-add), *meta*-addition (*m*-add) and *ipso*-addition (*ipso*-add) shown in Fig. 1 are OH-addition reactions. The ·OH radical attacks a ring carbon with its unpaired electron and upon contact forms a C—O bond, while a π-bond of the aromatic system is broken and a dihydroxychlorocyclohexadienyl type radical is formed. The fourth reaction path, H-abstraction (H-abs) is hydrogen abstraction from the functional —OH group producing 4-chlorophenoxyl radical and a water molecule. The process H-abstraction by the OH radical is a simple atom-transfer reaction in which the bond to the hydrogen atom in the —OH group is broken and a new bond to the oxygen atom of the ·OH radical is formed.

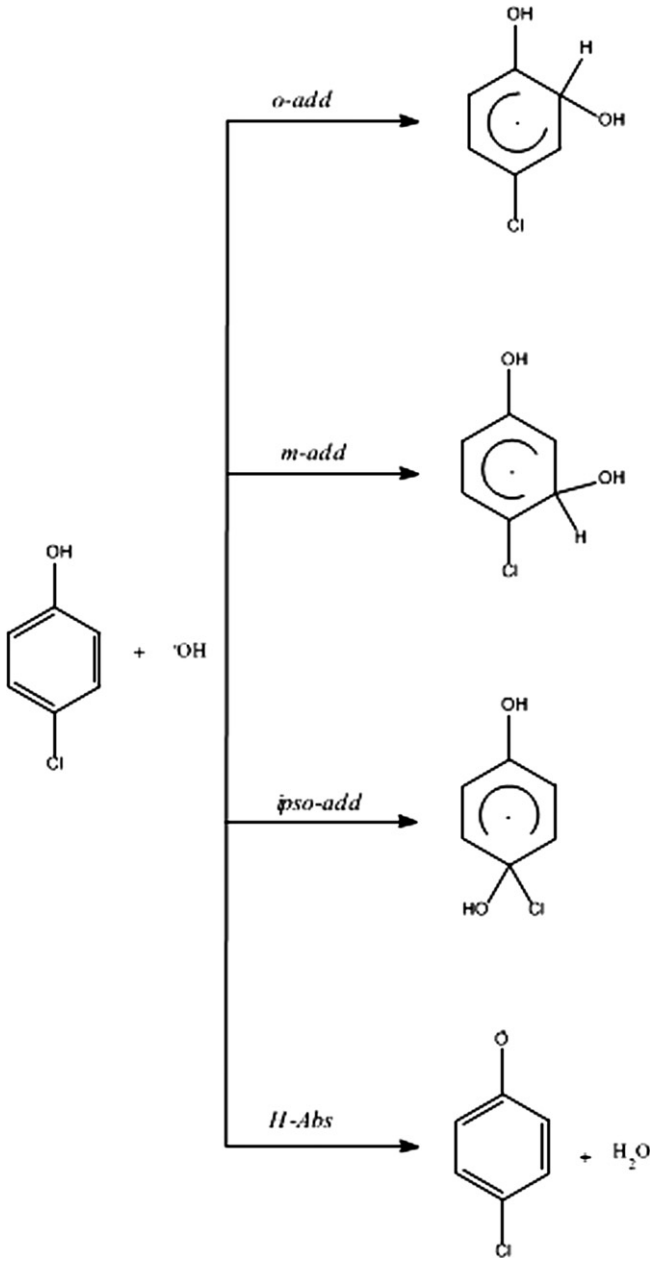

Fig. 1. Possible reaction paths for 4-CP + ·OH reaction.

3.2. Reactants and product radicals

Four different radicals were determined as the products of the reaction between 4-CP and the ·OH radical. The structures of the reactants and the product radicals were fully optimized. The optimized structures of the *o*-R and *ipso*-R radicals formed in the *ortho*- and *ipso*-addition paths are displayed in Fig. 2. The electronic and thermodynamic properties for the most stable conformers were also calculated. The total energies *E* for each of the reactants and the product radicals obtained for both gas and aqueous media are presented in Table 1.

The values in Table 1 indicate that the radicals, *o*-R, *m*-R and *ipso*-R produced in the addition paths are more stable than the one H-R produced in the abstraction path. The reason may be attributed to the fact that all the radicals produced in the addition paths have hydrogen-bond-like stabilizations as shown in Fig. 2. The interaction distance between the original hydrogen atom at the addition center and the oxygen atom of the added ·OH was calculated to be around 1.985 Å for *o*-R and *m*-R. As for the *ipso*-R, the high stability arises from the attraction between

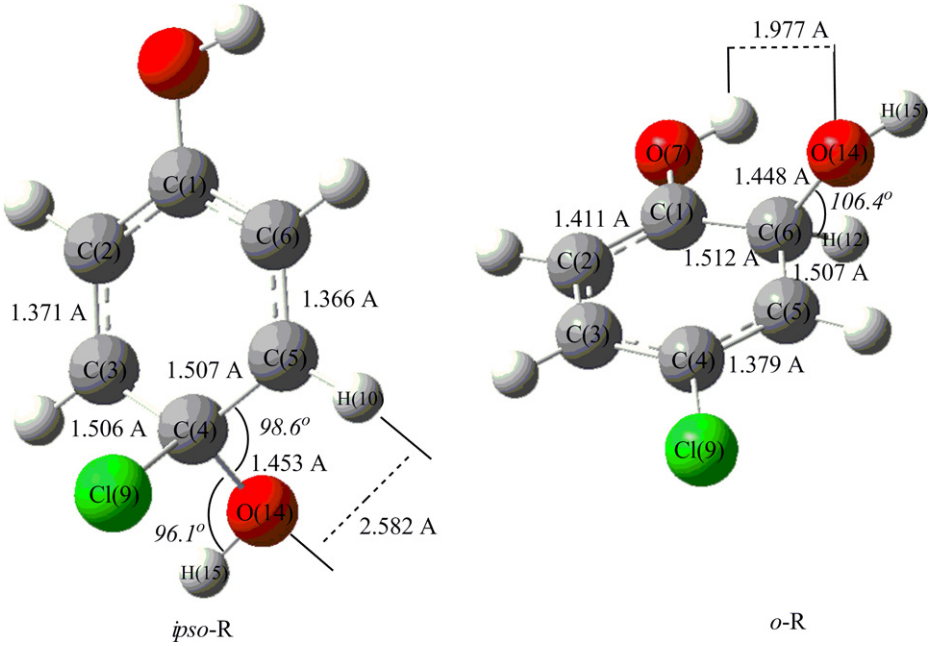

Fig. 2. The optimized structures of *o*-R and *ipso*-R radicals (grey: carbon, white: hydrogen, red: oxygen, green: chlorine) (For interpretation of the references to colour in this figure legend, the reader is referred to the web version of this article.)

Table 1
Energetic parameters for the reactants, product radicals, pre-reactive and transition state complexes

	E^{a}(Hartrees)	
	Gas phase	Aqueous phase
Reactants		
4-CP	−767.06036	−767.07648
OH	−75.72298	−75.73322
Product radicals		
o-R	−842.81539	−842.83349
m-R	−842.80925	−842.83009
ipso-R	−842.82240	−842.84872
H-R	−766.42411	−766.43475
Pre-reactive complexes		
o-PC	−842.80629	−842.83054
m-PC	−842.79886	−842.82459
ipso-PC	−842.80495	−842.82998
H-PC	−842.79819	−842.82421
Transition state complexes		
o-TS	−842.79923	−842.82402
m-TS	−842.78756	−842.81361
ipso-TS	−842.79689	−842.82261
H-TS	−842.78179	−842.80825

[a] Zero point corrected energies.

the hydrogen atom of the adding ·OH and the chlorine atom, the interaction distance was calculated to be 2.74 Å. For the gas phase, among the three radicals produced in the addition paths, *ipso*-R radical having the lowest energy is the most stable radical. The *o*-R is around 4 kcal mol^{-1} and the *m*-R is around 8 kcal mol^{-1} less stable than the *ipso*-R. The energy of H—R radical is too high to be compared with the energies of the addition radicals. For the aqueous phase, the sequence remains the same. The most and the least stable radicals are again the *ipso*-R and the H—R, respectively. However, all the product radicals are more stable in aqueous phase due to the effect of water molecules. The stabilities of the *o*-R and the *m*-R radicals increase by around 12 kcal mol^{-1} whereas the energy of the *ipso*-R radical decreases by around 17 kcal mol^{-1} in aqueous media. On the other hand, the difference in the gas and aqueous phase energies for the H—R was calculated to be 7 kcal mol^{-1}, much less than the former ones.

By using the localization approach of Wheland's approximation [27], it may be predicted that ·OH addition is the most probable reaction path and that the position of attack of the ·OH radical is the *ipso* position for both gas and aqueous phases, causing the chlorine atom to leave the molecule first in the photocatalytic degradation of 4-CP. As seen in Fig. 3, the products of the three addition paths lie. ca. 20 kcal mol^{-1} below the reactants. Hence, it may be concluded that the reactions will proceed to the corresponding products, once the reactants are sufficiently close to each other. The thermodynamically most favored product is 1,4-dihydroxy-4-chlorocyclohexadienyl radical followed by 1,2-dihydroxy-4-chlorocyclohexadienyl radical for gas and aqueous phases.

3.3. Pre-reactive complexes

Our DFT calculations for 4-CP + ·OH reaction resulted in negative activation energies for the four possible reaction paths. This finding indicates the formation of weakly-bound complexes between the ·OH radical and

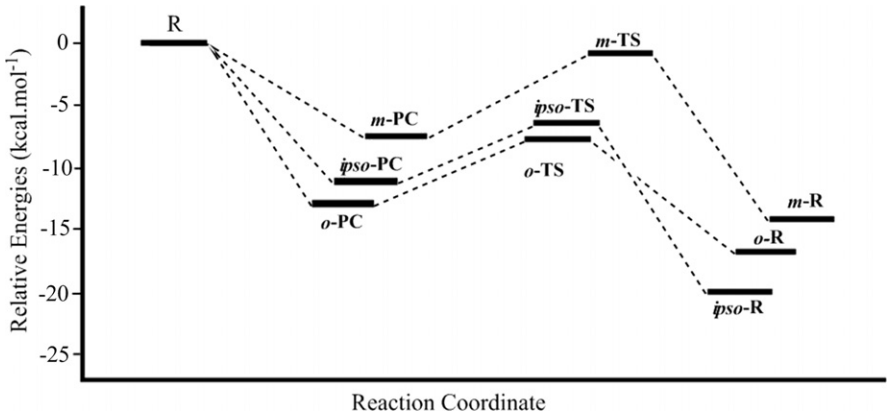

Fig. 3. Energy surfaces for the addition paths.

the aromatic molecule as the precursors to the reactions. Therefore, the reaction paths under investigation can not be considered as simple barrierless paths, but rather they proceed over barriers that are lower in energy than the reactants due to the existence of pre-reactive van der Waals complexes. These complexes exert strong influence over the kinetics of the reactions by altering barrier heights and/or affecting the energy partitioning of reaction products. Furthermore, the presence of such complexes also have a significant effect on the dynamics of the reaction by spatially directing the site of the reaction, either by steric direction or by favoring a reaction site by providing a low potential energy well.

Four different chemically activated pre-reactive complexes, *o*-PC, *m*-PC, *ipso*-PC and H-PC with shallow wells, ca. 12 kcal mol^{-1} which then form the product radicals were determined for the 4-CP + ·OH reaction for both gas and aqueous phases. The structures of all the complexes were fully optimized. Fig. 4 shows the optimized structures of the *o*-PC and the *ipso*-PC pre-reactive complexes. The total energies obtained for each of the pre-reactive complexes are presented in Table 1.

The major geometric changes in the pre-reactive complexes are located around the atom to which the oxygen atom of the ·OH radical is bound. The ring carbons connected to the oxygen atom of the ·OH were found to deviate from the ring plane by around 3° angle. The oxygen atom comes from the top of the ring making a 100–110° angle with the ring plane. The main difference in the optimized geometries displayed in Fig. 4 occurs in the distance between the oxygen atom of the ·OH and the ring carbon. *o*-PC has a much longer distance as compared with 2.38 Å in *m*-PC and 2.62 Å in *ipso*-PC. Energetically the *o*-PC is the most stable of the four, lying 14.4 kcal mol^{-1} below the isolated reactants. The *ipso*-PC is around 1 kcal mol^{-1} less stable, the *m*-PC and the H-PC are around 5 kcal mol^{-1} less stable than the *o*-PC. The least stable pre-reactive complex is the H-PC which is formed in the abstraction reaction. However, the stability of the *m*-PC is almost the same with the H-PC, the difference was found

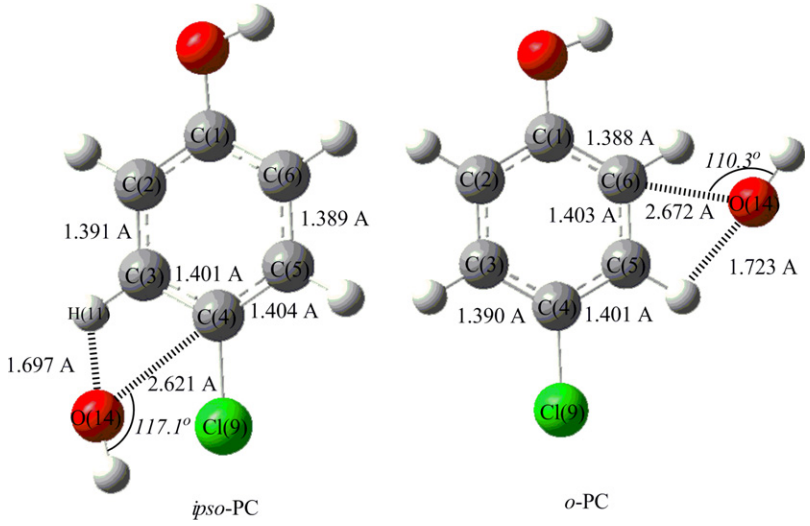

Fig. 4. The optimized structures of the *o*-PC and the *ipso*-PC pre-reactive complexes. (grey: carbon, white: hydrogen, red: oxygen, green : chlorine) (For interpretation of the references to colour in this figure legend, the reader is referred to the web version of this article.)

to be only 0.42 kcal mol^{-1}. Moreover, it was also observed that the stability of the pre-reactive complexes is higher in aqueous phase than in gas phase. For all the four complexes the energy difference was calculated to be around 2 kcal mol^{-1}.

3.4. Transition state complexes

Four transition state complexes *o*-TS, *m*-TS, *ipso*-TS and H-TS, one for each of possible reaction paths, were identified. The optimized structures of the *o*-TS and *ipso*-TS are displayed in Fig. 5. In all the complexes the OH group is oriented such that the oxygen atom comes from the top of the ring making a 117° angle with the plane of the ring for *o*-TS, 104° for *m*-TS, 51° for *ipso*-TS and 96° for H-TS, respectively. The hydrogen atom of the ·OH radical points towards the exterior part of the ring in *o*-TS, *ipso*-TS and H-TS, while in the *m*-TS it points towards the interior part of the ring. In the *o*-TS the phenolic hydrogen H10 rotates out of the ring plane by 10.8° to form a hydrogen bond to the adding oxygen O14. The interaction distance between H10 and O14 was calculated to be 1.949 Å. The hydrogen atom at the addition center rotates out of the ring plane to the opposite side of the OH by 8.2°. In the *m*-TS the original hydrogen atom at the addition center rotates by 10.1° to form a hydrogen bond with the oxygen atom of the OH. Whereas phenolic hydrogen rotates out of the ring plane by only 2°. In the *ipso*-TS chlorine atom rotates by 18.2° to the back side of the ring due to the repulsive effect of the oxygen atom of the ·OH radical.

In the addition paths the major structural changes in the ring geometry relative to the parent 4-CP molecule are all localized around the carbon atom to which the ·OH radical attacks. The two C—C bonds connecting the addition center lengthen by 0.03–0.04 Å, whereas the change in the bond lengths of the subsequent C—C bonds is less, around −0.01 Å. This finding indicates that the two C—C bonds connecting the addition center have single rather than double bond character. The ones away from the addition center have a more pronounced double bond character. In the abstraction complex H-TS all the geometric changes are located around the phenolic group and the carbon atom connecting it. Since a new bond is being formed between the phenolic hydrogen and the oxygen atom of the ·OH radical, C1—O7—H10 angle widens by 7°. There is also a slight elongation in the breaking bond, around 0.08 Å. Furthermore it was also observed that the phenolic hydrogen H10 rotates out of the ring plane by 41.2°.

The forming bond length is a sensitive measure of the formation of the transition state complex along the reaction coordinate. As displayed in Fig. 5, the addition complexes have much longer C—O bonds as compared to the C—O bonds in the corresponding radicals 1.45 Å. This suggests that the addition complexes are early transition states, whereas, the abstraction complex forms late along the reaction coordinate. Among the three addition complexes the longest C—O bonds belong to the *o*-TS and *ipso*-TSs, while the *m*-TS has a much shorter C—O bond indicating that it forms late along the reaction coordinate. Furthermore, the *o*-TS and the *ipso*-TS were found to have the lowest total energies among all the possible transition states (Table 1). The two TS complexes lie 9.98 and 8.51 kcal mol^{-1} below the reactants, respectively. The *m*-TS was found to have ca. 2 kcal mol^{-1} less energy than the reactants, whereas H-TS lies 0.96 kcal mol^{-1} higher than the reactants. It was observed that the sequence does not change in aqueous phase; however the energies of all the transition state complexes decrease by around 16 kcal mol^{-1} due to the effect of water molecules. The *o*-TS is the most thermodynamically

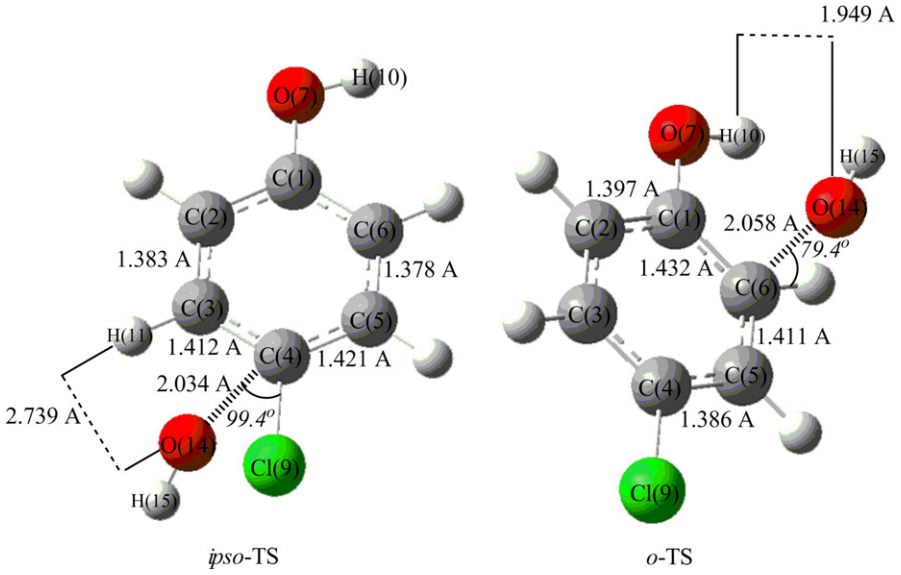

Fig. 5. The optimized structures of the *ipso*-TS and the *o*-TS. (grey: carbon, white: hydrogen, red: oxygen, green: chlorine) (For interpretation of the references to colour in this figure legend, the reader is referred to the web version of this article.)

stable TS for the aqueous phase. Thus we may conclude that the *o*-TS is the most probable transition state structure.

3.5. Energetics of the reaction paths

The activation energies E_a for the four possible reaction paths were calculated and presented in Table 2 together with the heats of reaction ΔH_r for both gas and aqueous phases. The values in Table 2 show that the activation energies for the three OH-addition paths are lower than the one for the H-abstraction path. The lowest activation energy belongs to the *ortho*-addition path. The energy barrier for the *ipso*-addition path is 0.63 kcal mol^{-1} higher than the energy barrier for the *ortho*-addition path. In aqueous phase, the difference in the barriers of the two paths decreases to 0.53 kcal mol^{-1}. On the other hand, the energy barriers for the *meta*-addition path were found to be 2.66 and 2.80 kcal mol^{-1} higher than the energy barriers for the *ortho*-addition path in gas and aqueous phases, respectively.

The difference in the energy barriers for the addition paths can be explained by the features of the pre-reactive complexes and the transition states. All the transition state complexes show hydrogen-bond-like stabilizations as shown in Fig. 5. The corresponding interaction distances are 1.949 Å for *o*-TS, and 2.157 Å for *m*-TS. Generally the shorter interaction distances cause larger stabilizations and lower energy barriers. Thus, the longer interaction distance in the latest one causes an increase in the energy barrier. Moreover, *ortho*- and *ipso*-addition paths were found to have the highest exothermicities. The result is consistent with Hammond's postulate [28] which states that early transition states have low energy barriers and high exothermicities. So, it may be concluded that *o*-TS and *ipso*-TS are the most probable transition states in accordance with the former predictions. The H-abstraction path has the highest activation energy so that H-TS is the least probable transition state. Moreover, the heat of reaction for the H-abstraction is highly endothermic in gas and aqueous phases.

3.6. Rate constants and product distribution

The rate constant k for each reaction path was calculated by using the Transition State Theory for 300 K. The classical rate constant k in the Transition State Theory is given by Eq. (1):

$$k = \frac{k_B T}{h} \frac{q_{TS}}{q_{4-CP} \cdot q_{OH}} e^{-E_a/RT} \quad (1)$$

where k_B is Boltzmann's constant, T is temperature, h is Planck's constant and q's are the molecular partition functions for TS and the reactant species, 4-CP and ·OH and E_a is the activation energy. Each of the molecular partition functions was assumed to be the product of translational, rotational, vibrational and electronic partition functions of the corresponding species. The calculated rate constants at ambient temperature 300 K are presented in Table 3.

The values in Table 3 show that the highest rate constant belongs to *o*-addition, followed by *ipso*- and *m*-addition, whereas H-abstraction is the slowest reaction path, consistent with its high energy barrier. The branching ratio for each of the reaction paths was calculated by dividing the corresponding rate constant by the sum of the rate constants taking the number of similar addition centers into account. By using the branching ratios, the relative concentrations of the primary intermediates were also calculated; they are presented in Table 4. The results indicate that *o*-addition is the dominant reaction path, followed by *ipso*-addition.

The product distribution obtained in this study shows that the major primary intermediate that is formed in the photocatalytic degradation of 4-CP is the *o*-R (1,2-dihydroxy-4-chlorocyclohexadienyl) radical which then forms 4-chlorocatechol as shown in Table 4. The reaction also yields the *ipso*-R (1,4-dihydroxy-4-chlorohexadienyl) radical through *ipso*-addition to the aromatic ring. As the chlorine substituent is then released due to the presence of water molecules and steric effects, the *ipso*-R is then converted to hydroquinone. Since, 4-chlorophenoxyl is the

Table 2
Activation energies E_a and heats of reaction ΔH_r for the reaction paths

Path	E_a (kcal mol^{-1})		ΔH_r (kcal mol^{-1})	
	Gas phase	Aqueous phase	Gas phase	Aqueous phase
o-Addition	4.43	4.09	−20.61	−23.37
m-Addition	7.09	6.89	−19.34	−23.24
ipso-Addition	5.06	4.62	−21.06	−24.73
H-Abstraction	10.29	10.02	Endothermic	Endothermic

Table 3
Rate constants k for the reaction paths

Path	k (cm^3 molecule^{-1} s^{-1})	
	Gas phase	Aqueous phase
o-Addition	9.39×10^{-13}	9.77×10^{-13}
m-Addition	9.64×10^{-15}	2.01×10^{-14}
ipso-Addition	5.63×10^{-13}	5.78×10^{-13}
H-Abstraction	3.34×10^{-21}	3.79×10^{-21}

Table 4
Product distribution for the reaction of 4-CP with ·OH radicals

Reaction path	Primary intermediate	Relative concentration	
		Gas phase	Aqueous phase
o-Addition	1,2-Dihydroxy-4-chlorobenzene	76.33	77.05
m-Addition	1,3-Dihydroxy-4-chlorobenzene	0.78	0.16
ipso-Addition	1,4-Dihydroxy-4-chlorobenzene	22.88	22.79
H-Abstraction	4-Chlorophenoxyl radical	0.00	0.00

least probable one, we conclude that polyaromatic compounds do not form in the photocatalytic degradation of 4-CP. Moreover, the rate constants in Table 3 show that all the reaction paths proceeds faster in aqueous phase, in consistence with the decrease in the activation energies. The results obtained in this study indicate that the major intermediates of the 4-CP + ·OH reaction are 4-chlorocatechol (4-CC) and hydroquinone (HQ) with [4-CC] > [HQ], confirming the experimental findings of earlier studies reported in the literature [12,13,29,30]. In several other studies, the amount of HQ formed relative to the amount of 4-CC has been found to be greater in photocatalysis. The reason may be attributed to the different adsorption capacities of the two compounds on TiO_2 particles, especially at high photocatalyst loadings [13].

4. Conclusions

1. Photocatalytic degradation of 4-CP may be based on hydroxyl radical chemistry.
2. Pre-reactive complexes are formed between the ·OH radical and 4-CP as the precursors to the reaction. The *o*-PC is the most stable pre-reactive complex, lying 14.4 kcal mol^{-1} below the isolated reactants.
3. In 4-CP + ·OH reaction, *ipso*-R radical produced by the addition of OH to the *ipso* carbon is the most stable radical.
4. The activation energies for the addition paths are lower than the one for the abstraction path due to hydrogen bonds. *o*-TS and *ipso*-TS are the most probable transition states.
5. The highest rate constant belongs to *ortho*-addition, followed by *ipso*- and *meta*- addition, whereas H-abstraction is the slowest reaction path.
6. The major intermediates of the 4-CP + ·OH reaction are 4-chlorocatechol (4-CC) and hydroquinone (HQ) with [4-CC] > [HQ].
7. The energies of all the species involved in 4-CP + ·OH reaction decrease in aqueous phase due to the effect of water molecules. Thus, the reaction paths proceed faster in aqueous media than in gas phase.

References

[1] Y. Pi, L. Zhang, J. Wang, J. Hazard. Mater. 141 (2007) 707–712.
[2] Y.T. Wei, Y.Y. Wang, C.Wan, J. Photochem. Photobiol. A: Chem. 55 (1990) 115–126.
[3] J.C. D'Oliveira, G. Al-Sayyed, P. Pichat, Environ. Sci. Technol. 24 (1990) 990–996.
[4] T. Pandiyan, O. Martines Rivas, J. Orozco Martines, G. Burillo Amezcua, M.A. Martinez-Carrillo, J. Photochem. Photobiol. A: Chem. 146 (2002) 149–155.
[5] A. Mills, S.L. Hunte, J. Photochem. Photobiol. A: Chem. 108 (1997) 1–35.
[6] D. Bahnemann, J. Cunningham, M.A. Fox, E. Pelizzetti, P. Pichat, N. Serpone, in: G.R. Helz, R.G. Zepp, D.G. Crosby (Eds.), Aquatic and Surface Photochemistry, Lewis, Baco Raton, FL, 1994, p. 261.
[7] P. Pichat, in: G. Ertl, H. Knözinger, J. Weitkamp (Eds.), Handbook of Heterogeneous Photo-Catalysis, vol. 4, VCH, Weinheim, 1997, p. 2111.
[8] J.C. D'Oliveira, C. Minero, E. Pelizzetti, P. Pichat, J. Photochem. Photobiol. A: Chem. 72 (1993) 261–267.
[9] K.H. Wang, Y.H. Hsieh, M.Y. Chou, C.Y. Chang, Appl. Catal. B: Environ. 21 (1999) 1–8.
[10] Y.C. Chan, J.N. Chen, M.C. Lu, Chemosphere 45 (2001) 29–35.
[11] A.M. Peiro, J.A. Ayllon, J. Peral, X. Domenech, Appl. Catal. B: Environ. 30 (2001) 359–373.
[12] U. Stafford, K.A. Gray, P. Kamat, J. Catal. 167 (1997) 25–32.
[13] U. Stafford, K.A. Gray, P.V. Kamat, J. Phys. Chem. 98 (1994) 6343–6351.
[14] A. Mills, J. Wang, J. Photochem. Photobiol. A: Chem. 118 (1998) 53–63.
[15] X. Li, J.W. Cubbage, T.A. Tetzlaff, W.S. Jenks, J. Org. Chem. 64 (1999) 8509–8524.
[16] X. Li, J.W. Cubbage, W.S. Jenks, J. Org. Chem. 64 (1999) 8525–8536.
[17] M. Kılıç, G. Koçtürk, N. San, Z. Çınar, Chemosphere 69 (2007) 1396–1408.
[18] Gaussian 03, Revision B.01, M.J. Frisch, G.W. Trucks, H.B. Schlegel, G.E. Scuseria, M.A. Robb, J.R. Cheeseman, J.A. Montgomery, Jr., T. Vreven, K.N. Kudin, J.C. Burant, J.M. Millam, S.S. Iyengar, J. Tomasi, V. Barone, B. Mennucci, M. Cossi, G. Scalmani, N. Rega, G.A. Petersson, H. Nakatsuji, M. Hada, M. Ehara, K. Toyota, R. Fukuda, J. Hasegawa, M. Ishida, T. Nakajima, Y. Honda, O. Kitao, H. Nakai, M. Klene, X. Li, J.E. Knox, H.P. Hratchian, J.B. Cross, C. Adamo, J. Jaramillo, R. Gomperts, R.E. Stratmann, O. Yazyev, A.J. Austin, R. Cammi, C. Pomelli, J.W. Ochterski, P.Y. Ayala, K.Morokuma, G.A. Voth, P. Salvador, J.J. Dannenberg, V.G. Zakrzewski, S. Dapprich, A.D. Daniels, M.C. Strain, O. Farkas, D.K. Malick, A.D. Rabuck, K. Raghavachari, J.B. Foresman, J.V. Ortiz, Q. Cui, A.G. Baboul, S. Clifford, J. Cioslowski, B.B. Stefanov, G. Liu, A. Liashenko, P. Piskorz, I. Komaromi, R.L. Martin, D.J. Fox, T. Keith, M.A. Al-Laham, C.Y. Peng, A. Nanayakkara, M. Challacombe, P.M.W. Gill, B. Johnson, W.Chen, M.W. Wong, C. Gonzalez, and J.A. Pople, Gaussian, Inc., Pittsburgh PA, (2003).
[19] A.D. Becke, J. Chem. Phys. 98 (1993) 5648–5652.
[20] C. Lee, W. Yang, R.G. Parr, Phys. Rev. B 37 (1988) 785–789.
[21] J.P. Stewart, J. Comput. Chem. 10 (1989) 209–220.
[22] J.P. Stewart, J. Comput. Chem. 10 (1989) 221–264.
[23] V. Barone, M. Cossi, J. Phys. Chem. A 102 (1998) 1995–2001.
[24] J. Andzelm, C. Kölmel, A. Klamt, J. Chem. Phys. 103 (1995) 9312–9320.
[25] N.S. Hush, J. Schamberger, G.B. Bacskay, Coord. Chem. Rev. 249 (2005) 299–311.
[26] M. Kılıç, N. San, Z. Çınar, J. Adv. Oxid. Technol. 10 (2007) 60–66.
[27] M.K. Eberhardt, M. Yoshida, J. Phys. Chem. 77 (1973) 589–597.
[28] W.J. Hehre, L. Radom, P.R. Schleyer, J.A. Pople, Ab Initio Molecular Orbital Theory, Wiley, New York, 1986.
[29] A. Mills, S. Morris, R. Davies, J. Photochem. Photobiol. A: Chem. 70 (1993) 183–191.
[30] A. Mills, S. Morris, J. Photochem. Photobiol. A: Chem. 71 (1993) 75–83.